



# Preparation and properties of flexible flame-retardant neutron shielding material based on methyl vinyl silicone rubber



Hao Chai<sup>a</sup>, Xiaobin Tang<sup>a,b,\*</sup>, Minxuan Ni<sup>a</sup>, Feida Chen<sup>a</sup>, Yun Zhang<sup>a</sup>, Da Chen<sup>a,b</sup>, Yunlong Qiu<sup>c</sup>

<sup>a</sup>Department of Nuclear Science & Engineering, Nanjing University of Aeronautics and Astronautics, Nanjing, China

<sup>b</sup>Jiangsu Key Laboratory of Nuclear Energy Equipment Materials Engineering, China

<sup>c</sup>ZhongXing Energy Equipment Co., LTD, Haimen Nantong, China

## ARTICLE INFO

### Article history:

Received 4 April 2015

Accepted 28 April 2015

Available online 6 May 2015

## ABSTRACT

Flexible flame-retardant composites were prepared using high-functional methyl vinyl silicone rubber matrix with B<sub>4</sub>C, hollow beads, and zinc borate (ZB) as filler materials. As filler content increased, the tensile strength, elongation, and tear strength of the composites initially increased and then decreased. The shore hardness of the composites increased with increasing filler content with a maximum value of 30 HA. The heat insulation properties of the composites with hollow beads were higher than that of the ordinary composites with the same filler mass fraction. When ZB content exceeded 12 wt%, the limit of oxygen index of the composites was higher than 27.1%. With Am–Be neutron as the test radiation source, the transmission of neutron for a 2 cm sample was only 47.8%. Powder surface modification improved the mechanical properties, thermal conductivity, flame retardancy, and neutron shielding performance of the composites, but did not affect shore hardness.

© 2015 Elsevier B.V. All rights reserved.

## 1. Introduction

Neutron is extensively applied in nuclear power, imaging technology, activation analysis, and radiotherapy [1–3]. As unwanted radiation is harmful to man and the environment, the demand for reliable neutron shielding materials has been increasing. Polymer composites containing <sup>10</sup>B can effectively shield against neutron radiations; boron compounds are relatively cheap and exhibit excellent thermal neutron absorption because of the high thermal neutron absorption cross-section ( $\sigma = 760$  b) of <sup>10</sup>B atoms [4,5]. Many polymer/B<sub>4</sub>C composites, such as epoxy/B<sub>4</sub>C [6–9] and polyethylene/B<sub>4</sub>C [10–12], are used to fabricate neutron shielding materials. The resultant materials feature good mechanical properties, neutron shielding performance, and potential applications. Nevertheless, these materials are unsuitable for devices, such as neutron detectors and instruments with structural abnormality, which require additional shield in narrow spaces and around curved surfaces. Furthermore, these neutron shielding composites cannot effectively attached to irregular surfaces because of their high hardness. Hence, new flexible neutron shielding materials must be developed.

Several flexible neutron shielding materials have been investigated. Sukegawa et al. [13] fabricated a flexible heat resistant neutron shielding material and applied it around the port of a vacuum vessel as an additional shield; the developed material could be used for diagnostics and reduction of the neutron streaming of a superconducting tokamak device, such as JT-60SA. Sukegawa et al. [14] also investigated another flexible neutron shielding composite, which could function as an additional shield around the lid of the future fast reactor system and as a shielding material to prevent neutron streaming around the duct of the facility. A new SEBS/B<sub>4</sub>C flexible neutron shielding composite has also been reported [15]. Nevertheless, these developed flexible neutron shielding materials have no flame retardant properties. Thus, flexible flame-retardant neutron shielding composites must be developed to improve the resistance of nuclear equipment to fire risks.

In this study, a new flexible flame-retardant neutron shielding material was fabricated through powder surface modification, silicone rubber mixing, and vulcanized molding. Methyl vinyl silicone rubber (VMQ) was used as matrix, 2,5-dimethyl-2,5-di(tert-butyl peroxy) hexane (DBPH) as vulcanizing agent, B<sub>4</sub>C as neutron absorber, and zinc borate (ZB) as flame retardant. ZB not only exhibits good flame retardancy, but also increases B concentration and improve neutron shielding performance of the composites. Hollow bead materials (HBMs) were also added into the composites to enhance the heat insulation property of the product. The neutron shielding material features good flexible performance, excellent flame retardancy, and wide potential applications.

\* Corresponding author at: Department of Nuclear Science & Engineering, Nanjing University of Aeronautics and Astronautics, Nanjing, China. Tel.: +86 13601582233; fax: +86 025 52112906 80407.

E-mail address: [tangxiaobin@nuaa.edu.cn](mailto:tangxiaobin@nuaa.edu.cn) (X. Tang).

## 2. Experimental

### 2.1. Materials

The following materials were used to prepare a flexible flame-retardant neutron shielding material: B<sub>4</sub>C powder (>99%, ~50 μm, Sinopharm Reagent, China), ZB powder (2335, >99%, ~2 μm, Tianjin Guangfu Chemical Research Institute, China), HBM (SiO<sub>2</sub> > 75%, Al<sub>2</sub>O<sub>3</sub> > 12%, ~80 μm, Chongqing Aluo Technology Development Company Limited, China), silane coupling agent (KH-550, >99%, Chengguang Chemical, China), absolute ethyl alcohol (>99%, Nanjing Chemical Reagent Company Limited, China), oxalic acid dehydrate (>99.5%, Tianjin Fuchen Chemical Reagents Factory, China), VMQ (110-3S, Dongjue Silicone Group Company Limited, China), and DBPH (101, >93%, Shanghai Farida Chemical Company Limited, China).

### 2.2. VMQ composite fabrication

The surfaces of the fillers were modified to improve the interfacial adhesion between the VMQ matrix and the powder filler. Absolute ethyl alcohol, deionized water, and silane coupling agent (16:3:1 volume ratio) were added into a 1 L glass beaker reactor. Oxalic acid dehydrate was added into the mixture until the solution reached pH 3–4, and the mixture was hydrolyzed at room temperature for 1 h. The mixture was then added with filler particles and agitated at 60 °C for 5 h. Finally, the resulting slurry was filtered and dried at 110 °C for 3 h to obtain the surface-treated fillers.

The VMQ matrices and uncured VMQ composites were fabricated in a mixing mill. The VMQ matrices were prepared through mechanical mixing of VMQ and DBPH for 10 min with a mixing weight ratio of 100:1. The uncured VMQ composites were also prepared through mechanical mixing of VMQ matrices and filler powders for 15 min. The filler ingredients of the samples are summarized in Table 1.

The VMQ composite samples were fabricated through vulcanized molding with a plate vulcanizing machine. The uncured VMQ composites were placed into a mold coated with a release agent. The mold was pressed under 15 MPa by using a plate vulcanizing machine after the release cloths were covered. The VMQ composites were cured in the mold for 15 min at 170 °C. Finally, the VMQ composite samples were post-cured in a draught drying cabinet for 4 h at 200 °C. The flexible VMQ composite samples featured a plate-type structure with dimensions of 100 mm × 100 mm × 5 mm (Fig. 1). In the figure, the left sample is a neat VMQ and the right samples represent the VMQ composites with functional fillers.

### 2.3. Characterization

Surface-treated filler powders were examined through Fourier transform infrared (FTIR) spectrometry (Nicolet NEXUS-6700). The fracture surface morphology of the VMQ composites was observed through scanning electron microscopy (SEM, JSM-7500,

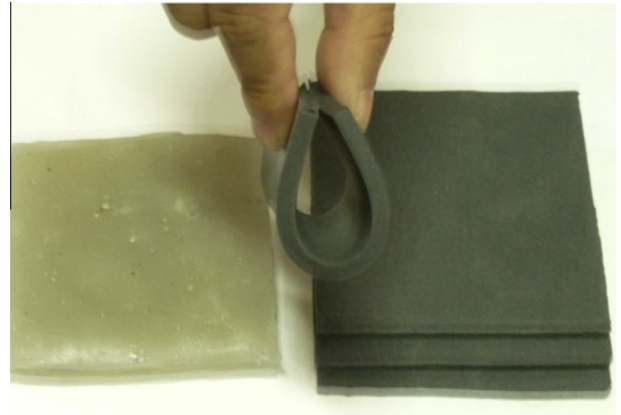


Fig. 1. Flexible VMQ composite samples.

JEOL). The mechanical properties of the VMQ composites were evaluated at room temperature by using a mechanical testing machine (WANCE ETM-D). Tensile (ASTM D412) tests were conducted at a strain rate of 500 mm/min, and tearing (ASTM D624) tests at 50 mm/min. Shore hardness tests were performed using a shore A durometer according to the ASTM D2240 standard. The thermal transmission properties of the VMQ composites were assessed using a thermal conductivity instrument (XIANGKE DRL-3) according to the ASTM D5470 standard. Flame resistance was evaluated by measuring the limit oxygen index (LOI) based on the ASTM D2863 standard. LOI is expressed as follows [16]:

$$\text{LOI} = 100 \frac{[\text{O}_2]}{[\text{O}_2] + [\text{N}_2]} \quad (1)$$

Radiation shielding characteristic was determined using thermal neutron transmission tests. Am–Be neutron, which was used as the test radiation source, was placed at the end of the cylindrical window-oriented detector side in the paraffin box. The cylindrical window was 130 mm deep and 110 mm wide. Neutron ray penetrated through a 30 mm-thick lead plate, passed through a polyethylene plate (30 mm thick) and VMQ composite samples (20 mm thick), and finally detected with an He-3 proportional counter. A schematic diagram of neutron shielding performance test is shown in Fig. 2.

## 3. Results and discussion

### 3.1. Surface characterization

FTIR spectroscopic measurements were performed to determine changes in the morphology of filler powders. Fig. 3 shows

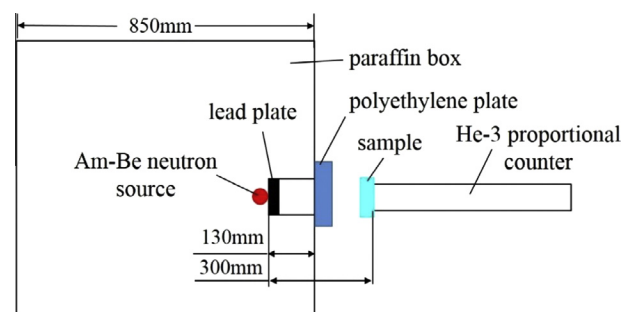


Fig. 2. Schematic diagram of neutron shielding performance test of the VMQ composites.

Table 1  
Compositions of different samples.

Sample No.	Material
1	Neat VMQ/DBPH
2	VMQ/DBPH (76.8 wt%) B <sub>4</sub> C (15 wt%) HBM (1.2 wt%) ZB (7 wt%)
3	VMQ/DBPH (61 wt%) B <sub>4</sub> C (25 wt%) HBM (2 wt%) ZB (12 wt%)
4	VMQ/DBPH (51.2 wt%) B <sub>4</sub> C (30 wt%) HBM (2.8 wt%) ZB (16 wt%)
5	VMQ/DBPH (41.5 wt%) B <sub>4</sub> C (35 wt%) HBM (3.5 wt%) ZB (20 wt%)
6	VMQ/DBPH (32.7 wt%) B <sub>4</sub> C (40 wt%) HBM (5.3 wt%) ZB (22 wt%)

the FTIR spectra of surface-modified and untreated filler powders. The three peaks at 472, 804, and 1109  $\text{cm}^{-1}$  changed compared with the FTIR spectrum of untreated fillers. The new peak appeared at 1620  $\text{cm}^{-1}$  after chemical treatment with silane coupling agent. The two peaks at 472 and 804  $\text{cm}^{-1}$  are assigned to the Si–O bond, whereas the two peaks at 1109 and 1620  $\text{cm}^{-1}$  are assigned to the Si–O–Si and  $-\text{NH}_2$  moieties, respectively. The increase in the absorption peaks of surface-modified fillers could be due to the superimposing absorption peaks of silane coupling agent and hydrolysis products on the inherent characteristic absorption peaks of the fillers. The changes in the peaks and appearance of new peaks indicate successful surface modification of filler powders.

### 3.2. Morphology observations

The fracture surfaces of the VMQ composites after tensile tests were investigated to determine the effect of surface modification on the interfacial adhesion and dispersion quality of the filler particles. Fig. 4(a) and (b) shows the SEM micrographs of the fracture surfaces of sample 2 with raw and surface-modified fillers, respectively. Fig. 4(c) and (d) represents the corresponding SEM micrographs of the fracture surfaces of sample 3 with raw and surface-modified fillers, respectively. Fig. 4(e) and (f) shows the SEM micrographs of the fracture surfaces of sample 4 with raw and surface-modified fillers, respectively. Fig. 4(g) and (h) shows the SEM micrographs of the fracture surfaces of sample 5 with raw and surface-modified fillers, respectively. Fig. 4(i) and (j) shows the SEM micrographs of the fracture surfaces of sample 6 with raw and surface-modified fillers, respectively. The filler contents of samples 2, 3, 4, 5 and 6 are summarized in Table 1. The composites with treated fillers in Fig. 4(b), (d), (f), (h) and (j) exhibited morphologies distinct from the composites with untreated fillers in Fig. 4(a), (c), (e), (g) and (i), respectively. Agglomerated fillers, interfacial voids and cracks are shown in Fig. 4(a), (c), (e), (g) and (i). This finding indicates the apparent poor dispersion properties and interfacial adhesion of the filler particles in the VMQ matrix. In Fig. 4(b), (d), (f), (h) and (j), the filler particles strongly adhered onto the VMQ matrix and the agglomerations are hardly observed on the fractured surfaces in the composites. From the SEM images, surface modification of the fillers apparently improved dispersion and adhesion in the VMQ matrix.

### 3.3. Mechanical properties

The mechanical properties of the radiation shielding materials are important in determining the material service conditions. The

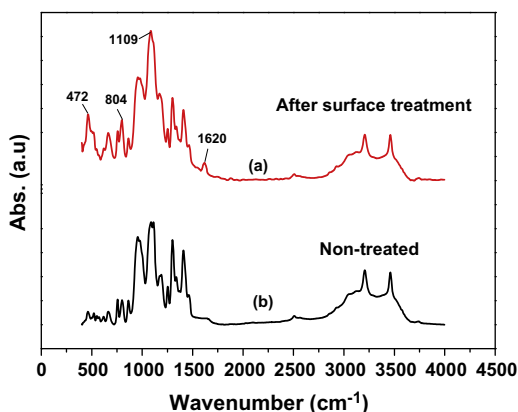
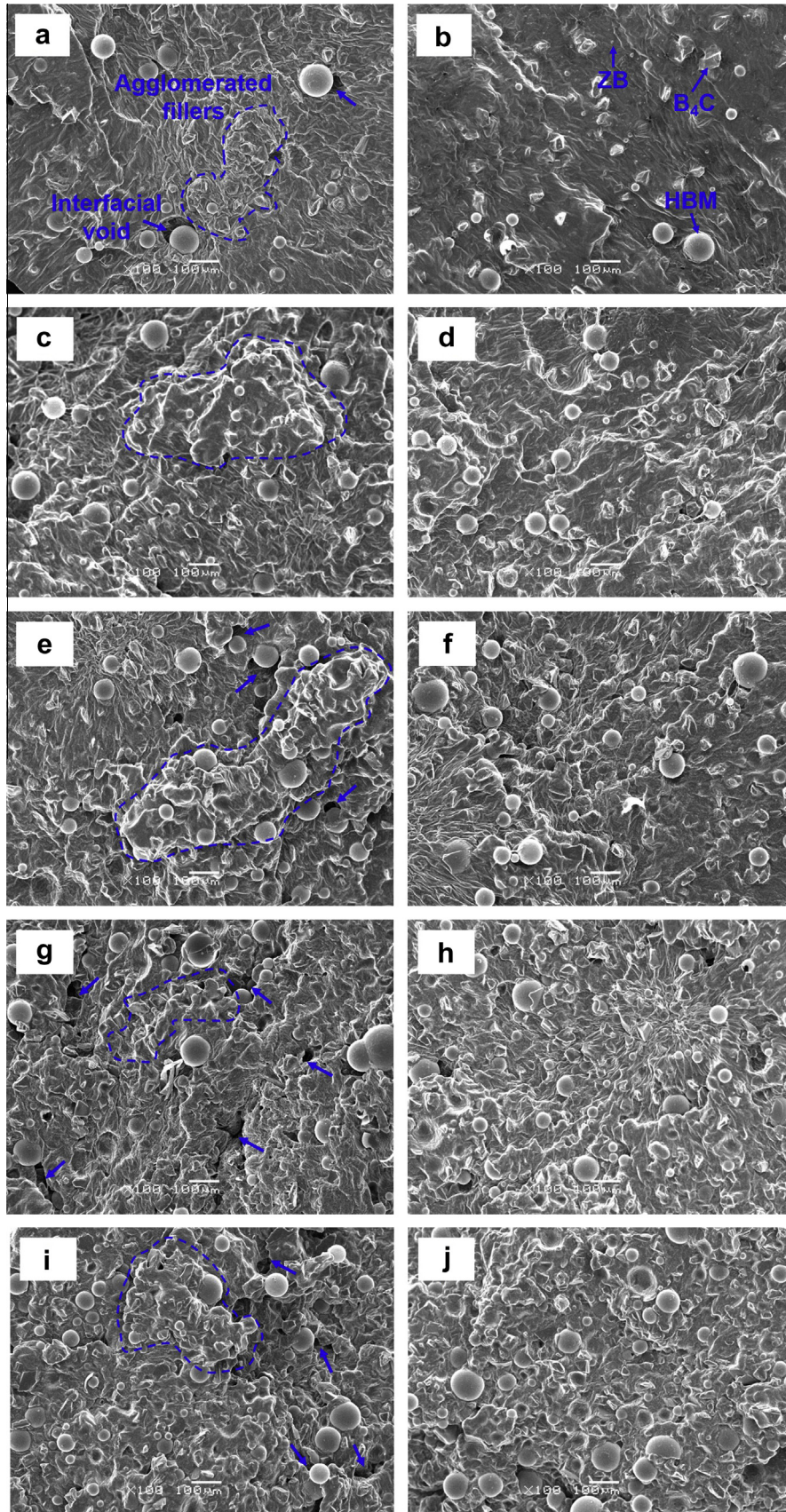


Fig. 3. FTIR spectra of surface-treated and untreated fillers.

mechanical properties of the VMQ-based neutron shielding materials with different filler contents at room temperature are shown in Fig. 5. The tensile properties of the composites were characterized by tensile strength and elongation at break. Fig. 5(a) and (b) shows the tensile strength and elongation of the modified and unmodified VMQ composites. As the filler concentration increased, the tensile strengths and elongations of both VMQ composites initially increased and then decreased. As addition of a small amount of filler powder in the matrix could reinforce the VMQ matrices, the tensile strengths and elongations of the VMQ composites increased. However, more defects in the matrix appeared when the filler content increased and the tensile strength and elongation of the composites were weakened by defects. The tensile strengths and elongations of the modified composites were higher than those of the unmodified composites because the adhesion and dispersion of the particles in the modified composites seemed to be stronger and more homogeneous. Fig. 5(c) shows the tear strengths of the modified and unmodified VMQ composites. With increasing filler content, the tear strengths of the composites initially increased and then decreased. This phenomenon could be attributed to the interfaces between particles and the capacity of the VMQ matrix to hinder crack extension upon addition of filler particles, thereby increasing the tear strength of the composites. However, the high levels of fillers caused by agglomerates, interfacial voids and cracks of the particles in the matrix damaged the continuous structure and formed stress concentration in the composites, resulting in weaker tear strength. The modified composites also enhanced tear strengths because the crack initiation and propagation along the interface might be inhibited by the enhanced particle/matrix interfacial adhesion. The modified composites showed a maximum tear strength of  $3.73 \pm 0.05$  KN/m; this strength which was higher than the tear strength of the unmodified composites ( $\sim 3.51 \pm 0.08$  KN/m). Fig. 5(d) shows the shore hardness that characterizes the flexibility of the composites. The filler content and hardness are important factors in the shore hardness of the composites. In this study, the VMQ material displayed low shore hardness but filler particles exhibited high shore hardness. Thus, the shore hardness of the VMQ composites increased with increasing filler content and filler surface modification almost did not influence the shore hardness of the VMQ composites. Sample 6 exhibited a maximum shore hardness of  $30 \pm 0.7$  HA, but the sample retained its flexibility.

### 3.4. Thermal conductivity

As radiation shielding materials exhibit excellent heat insulation performance and protect nuclear instruments against high temperature caused by fires, the thermal conductivity of these materials must also be evaluated. Fig. 6 shows the thermal conductivity of the neutron shielding composites. The thermal conductivity of the polymeric composites is mainly governed by the types and contents of particulate fillers. The thermal conductivity of the neat VMQ was  $0.27 \pm 0.01$   $\text{W m}^{-1} \text{K}^{-1}$ , and the thermal conductivities of the VMQ composites increased with increasing filler content as  $\text{B}_4\text{C}$  and ZB fillers exhibit high thermal conductivities. The composites with HBM showed lower effective thermal conductivities than those without HBM at the same filler content. When the HBM content exceeded 3.5 wt%, the thermal conductivities started to decrease. This phenomenon could be due to the lower thermal conductivity of HBM ( $0.05$   $\text{W m}^{-1} \text{K}^{-1}$ ) than those of the  $\text{B}_4\text{C}$  ( $17$   $\text{W m}^{-1} \text{K}^{-1}$ ), ZB ( $26$   $\text{W m}^{-1} \text{K}^{-1}$ ), and VMQ matrix. Nevertheless, the modified composites showed higher effective thermal conductivity than the unmodified composites at the same filler content. The surface modification of the fillers could be due to the alleviated phonon scattering at the interface of the VMQ matrix and filler particle compared with that of the unmodified composites. In most cases, the phonon



**Fig. 4.** SEM micrographs of the fractured surfaces of the VMQ composites: sample 2 with (a) raw and (b) treated filler powders; sample 3 with (c) raw and (d) treated filler powders; sample 4 with (e) raw and (f) treated filler powders; sample 5 with (g) raw and (h) treated filler powders; and sample 6 with (i) raw and (j) treated filler powders.

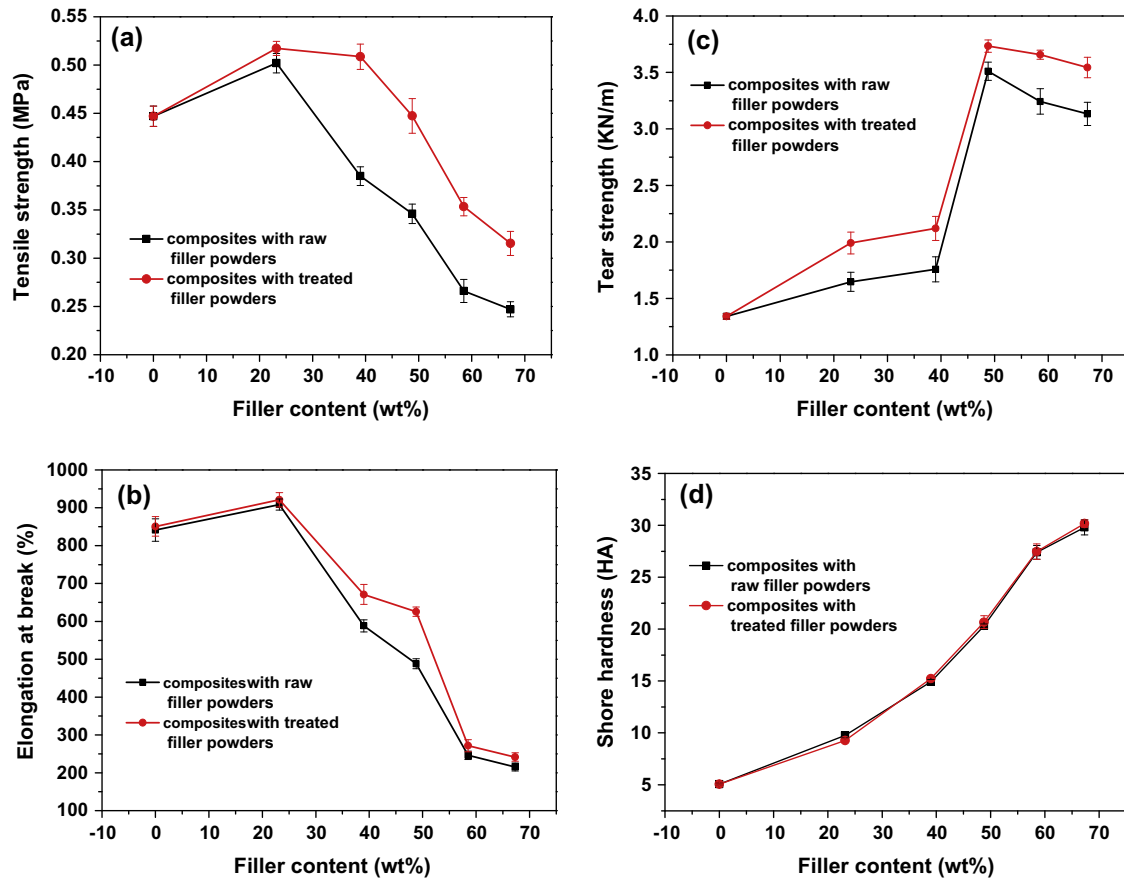


Fig. 5. Mechanical properties of the VMQ composites: (a) tensile strength, (b) elongation at break, (c) tear strength, and (d) shore hardness.

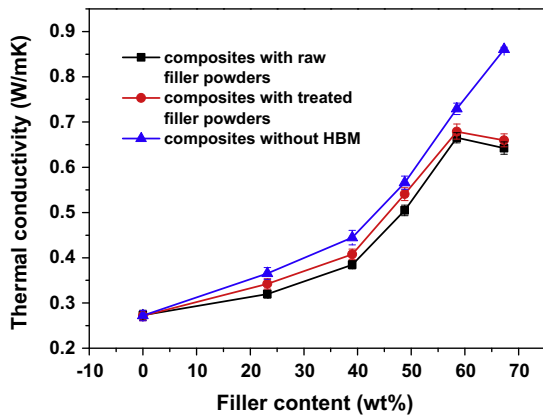


Fig. 6. Effective thermal conductivity versus filler content for composites with raw filler, treated filler, and without HBM.

scattering at the interface of the matrix/filler restricts heat transfer and the poor interfacial adhesion between the matrix and the filler leads to large phonon scattering [17]. In this work, we confirmed that HBM can efficiently reduce the thermal conductivity of the composites and provide applications for preparing heat-resistant materials.

### 3.5. Flame retardancy

Flame retardancy is an indispensable property of radiation materials and important in improving the fire resistance of nuclear

instruments and equipment. Metal hydroxide flame retardants are used to prepare flame-resistant materials because these retardants can release water vapor to remove heat from the flame and thus reduce the formation of combustible gases. In this study, the effects of 7 wt%, 12 wt%, 16 wt%, 20 wt%, and 22 wt% of ZB on flame retardant performance were investigated. ZB not only exhibits good flame retardancy, but can also increase B concentration and improve neutron shielding performance of the composites. The flame resistance of the composites was evaluated by measuring LOIs, and the results are shown in Table 2. The LOI for the neat VMQ material was 23%, which characterizes a combustible material. With increasing ZB content, the flame retardancies of the composites increased. The experimental results showed that the modified VMQ composites exhibited improved flame retardancy. The dispersion of the surface-modified ZB was homogeneous, thus improving the LOI for the composites by releasing water vapor evenly to dilute the air. When ZB content was higher than 12 wt%, the LOI of the composites was higher than 27.1% and reached the hardly flammable material grade. However, in most

Table 2  
LOIs of different samples.

Sample no.	ZB content (wt%)	LOIs for unmodified composites (%)	LOIs for modified composites (%)
1	0	23.0	23.0
2	7	24.3	24.6
3	12	26.5	27.1
4	16	29.4	29.9
5	20	32.2	32.8
6	22	34.1	34.8

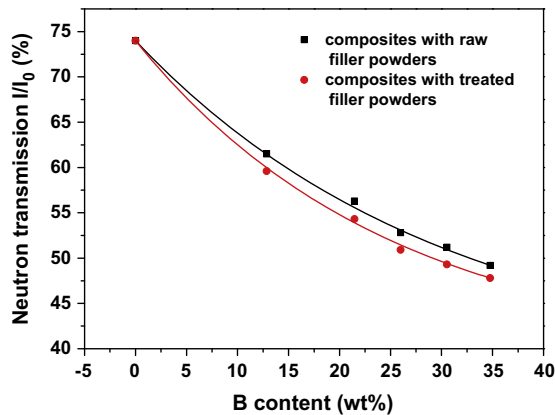


Fig. 7. Neutron transmission factor versus B content for composites with raw and treated fillers.

cases, a high loading of inorganic fillers, such as ZB, may adversely affect the mechanical strength of the composites [18].

### 3.6. Neutron radiation shielding properties

Finally, the neutron shielding characteristics of the modified and unmodified VMQ composites at various B contents were determined. The neutron transmission factor  $I/I_0$  was used to assess the neutron shielding properties, where  $I_0$  and  $I$  are the intensities of the incident neutron beam and neutron beam transmitted through the thickness direction of the sample composites, respectively. Fig. 7 shows the neutron flux attenuation properties of the 20 mm-thick VMQ composites. The neat VMQ material revealed an  $I/I_0$  value of 74%. With increasing B content, the transmission factor decreased. The modified composites exhibited enhanced neutron radiation shielding efficiency than the unmodified composites. The surface functionalization of  $B_4C$  and ZB strengthened the interfacial property of matrix/ $B_4C$  and matrix/ZB, and improved  $B_4C$  and ZB dispersion in the matrix, thereby effectively enhancing the neutron shielding ability. Consequently, high-performance neutron shielding composite materials need not only an excellent matrix and a neutron absorber, but also appropriate interfacial and dispersion properties between the components.

## 4. Conclusion

A new VMQ-based flexible-flame retardant neutron shielding composite was fabricated through powder surface modification, silicone rubber mixing, and vulcanized molding. Filler content and particle surface modification were evaluated to investigate the mechanical properties, thermal conductivity, flame retardancy, and neutron shielding performance of the composites. With increasing filler content, the tensile strength, elongation, and tear strength of the composites initially increased and then decreased. The shore hardness of the VMQ composites increased with increasing filler content with a maximum value of 30 HA, which was still

very flexible. The thermal conductivities of the VMQ composites also increased with increasing filler content. Addition of hollow beads (~5.3 wt%) resulted in 25.6% higher heat insulation properties of the composites than that of the ordinary composites with the same filler mass fraction. The flame retardancy of the VMQ composites was enhanced with increasing ZB content. When ZB content exceeded 12 wt%, the LOI of the composites was higher than 27.1% and reached the hardly flammable material grade. Am-Be neutron was used as the test radiation source, and the transmission of neutron for a 2 cm sample was only 47.8%. Particle surface modification improved the mechanical properties, thermal conductivity, flame retardancy, and neutron shielding properties of the composites, but shore hardness was not affected.

Therefore, the developed neutron shielding material features excellent flexibility, flame retardancy, heat insulation, neutron shielding performance, and extensive potential applications.

## Acknowledgements

This work was supported by the Project supported by the National Defense Basic Scientific Research Project (Grant No. B2520133007), the Project supported by the Cooperative Innovation Fund project of Jiangsu Province (Grant No. BY2014003-04), the Project supported by the Funding of Jiangsu Innovation Program for Graduate Education (Grant No. SJZZ\_0040), and the A Project Funded by the Priority Academic Program Development of Jiangsu Higher Education Institutions (PAPD).

## References

- [1] R. Zboray, R. Adams, M. Cortesi, H.M. Prasser, Nucl. Eng. Des. 273 (2014) 10–23.
- [2] Z. Revay, G. Kennedy, Radiochim. Acta 100 (2012) 687–698.
- [3] L. Evangelista, G. Jori, D. Martini, G. Sotti, Appl. Radiat. Isotopes 74 (2013) 91–101.
- [4] J. Jung, J. Kim, Y.R. Uhm, J.K. Jeon, S. Lee, H.M. Lee, C.K. Rhee, Thermochim. Acta 499 (2010) 8–14.
- [5] J. Kim, B.C. Lee, Y.R. Uhm, W.H. Miller, J. Nucl. Mater. 453 (2014) 48–53.
- [6] Y.P. Huang, W.J. Zhang, L. Liang, J. Xu, Z. Chen, Chem. Eng. J. 220 (2013) 143–150.
- [7] F.D. Chen, X.B. Tang, P. Wang, D. Chen, Atom. Energy Sci. Technol. 46 (2012) 703–707 (in Chinese).
- [8] J. Jun, J. Kim, Y. Bae, Y.S. Seo, J. Nucl. Mater. 416 (2011) 293–297.
- [9] H.S. Hu, Q.S. Wang, J. Qin, Y.L. Wu, et al., IEEE Trans. Nucl. Sci. 55 (2008) 2376–2384.
- [10] J.W. Shin, J.W. Lee, S. Yu, B.K. Baek, J.P. Hong, Y. Seo, W.N. Kim, S.M. Hong, C.M. Koo, Thermochim. Acta 585 (2014) 5–9.
- [11] C. Harrison, S. Weaver, C. Bertelsen, E. Burgett, N. Hertel, E. Grulke, J. Appl. Polym. Sci. 109 (2008) 2529–2538.
- [12] H. Courtney, B. Eric, H. Nolan, G. Eric, Ceram. Eng. Sci. Proc. 29 (2009) 77–84.
- [13] A.M. Sukegawa, Y. Anayama, K. Okuno, S. Sakurai, A. Kaminaga, J. Nucl. Mater. 417 (2011) 850–853.
- [14] A.M. Sukegawa, Y. Anayama, S. Ohnishi, S. Sakurai, A. Kaminaga, K. Okuno, J. Nucl. Sci. Technol. 48 (2011) 585–590.
- [15] H. Chai, X.B. Tang, F.D. Chen, D. Chen, Atom. Energy Sci. Technol. 48 (2014) 839–844 (in Chinese).
- [16] F. Laoutid, L. Bonnaud, M. Alexandre, J.-M. Lopez-Cuesta, Ph. Dubois, Mater. Sci. Eng. R 63 (2009) 100–125.
- [17] J.P. Hong, S.W. Yoon, T.S. Hwang, Y.K. Lee, S.H. Won, J.D. Nam, Korea-Aust. Rheol. J. 22 (2010) 259–264.
- [18] M.K. Lee, J.K. Lee, J.W. Kim, G.J. Lee, J. Nucl. Mater. 445 (2014) 63–71.